Korean J. Chem. Eng., **28**(11), 2130-2136 (2011)
DOI: 10.1007/s11814-011-0084-7

Pattern formation in drying of particle-laden sessile drops of polymer solutions on solid substrates

Yongjoon Choi, Jeongin Han, and Chongyoup Kim†

Department of Chemical and Biological Engineering, Korea University, Anam-dong, Sungbuk-gu, Seoul 136-713, Korea
(*Received 14 February 2011 • accepted 1 April 2011*)

Abstract–The drying of particle-laden sessile drops of water or polymer solutions was investigated experimentally. The contact angle of water on the solid surface was 45°. Particles used in the experiment were polystyrene particles of 1 and 6 μm and hollow glass spheres of 9-13 μm. As the polymers polyethylene oxide of 200 and 900 kDa and xanthan gum were used. Depending on particle size and fluid viscosity, the drying pattern varied and there was a competition of the inward movement due to the capillary and/or buoyant force acting on the particles trapped at the liquid interface and the outward movement due to the Deegan flow. The typical 'coffee ring' of colloidal particles was not always observed. Either inward or outward motion was observed depending on low shear viscosity. Elasticity does not appear to change the Deegan flow qualitatively. However, elasticity appears to change the pinning characteristics of the contact line.

Key words: Deegan Flow, Capillary Force, Low Shear Viscosity, Contact Line Pinning, Coffee Ring

INTRODUCTION

The drying of droplets with solid particles on solid substrate has important roles in many newly emerging fields such as micro-patterning of electronic devices [1], DNA chips [2], inkjet printing [3,4] and etching [5]. It has been well established that when a small drop of dilute colloidal suspension is dried on a wetted solid substrate, colloidal particles are accumulated at the contact line and a typical drying pattern, the so called 'coffee ring', remains. The reason for the formation of such a pattern is the contact line pinning due to the particles suspended in the liquid and the movement of particles and liquid together toward the rim to replenish the liquid that evaporates much faster near the contact line [6] (called the Deegan flow). Marangoni effect may act against the move toward the rim and results in the movement of particles toward the center of the drop [7,8]. The presence of a coffee ring pattern may or may not be desirable depending on the application. In the case of inkjet printing it gives a sharper image. In the case of printed electronics they usually require uniform deposition. Therefore, the control of drying pattern is very important in electronic and bio-industries.

There has been growing interest on drying characteristics of suspensions depending on the physicochemical characteristics of solid substrates and particles. Uno et al. [9] and Tay and Edirisinghe [10] reported that the hydrophilic nature of solid substrate affects the drying pattern. Recently Yan et al. [11] reported that electrostatic interaction between particle and substrate has a strong effect on colloidal self-assembly in a sessile drop, hence the drying pattern as a whole. Bhardwaj et al. [12,13] reported that, in the case of colloidal particles, the DLVO interaction between the particle and the solid substrate has a strong effect on drying patterns. Particle size can affect the drying pattern, too [14]. All of these studies have been limited to the drying of sessile drops of Newtonian fluids.

Although the flow inside the drop and heat transfer characteristics of Newtonian fluids with colloidal particles are relatively well understood through these studies, the flow and heat transfer characteristics of other kind of suspensions are poorly understood, particularly particle-laden non-Newtonian fluids and fluids with non-colloidal particles. However, most of the practically important systems such as inkjet systems [15] and colloidal processing of ceramics [16] are based on non-Newtonian liquids. This is because various polymers and surfactants are added to have the desired properties under flow and solidified conditions. Also, many practically important suspensions are made of particles with larger diameters. In this paper we report the experimental studies on the drying of particle-laden sessile drops of polymer solutions on glass substrates. Polyethylene oxide (PEO) and xanthan gum (XG) were chosen as the flexible and semiflexible chains to examine the effect of chain flexibility. The results show that dissolved polymer has a strong effect on drying pattern, and that the capillary force acting on the particles bound to the air-liquid interface also affects the drying pattern in the case of particles with large diameter.

EXPERIMENTAL

1. Materials

As the glass substrate we used amine-modified slide glasses purchased from GS Nanotech Inc. The self-assembled monolayer of 3-aminopropyltriethoxysilane is known to be prepared by dehydrating ethoxy-groups in 3-aminopropyltriethoxysilane. In hydroxyl solvents this surface is positively charged by the NH_3^+. The contact angle of water on this surface is approximately 45°. The liquids we examined were deionized water and aqueous solutions of xanthan gum (XG) and polyethylene oxide (PEO, MW: 200 kDa and 900 kDa). XG and PEOs were purchased from Sigma Aldrich Co. and used as received. Fig. 1 shows the rheological properties of the liquids

†To whom correspondence should be addressed.
E-mail: cykim@grtrkr.korea.ac.kr

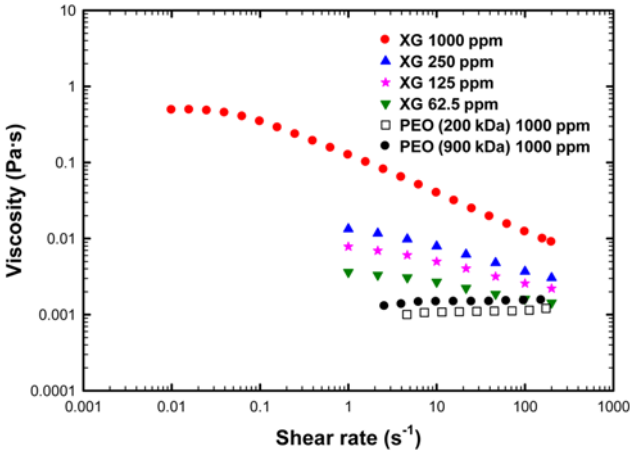

Fig. 1. The viscosities of 1,000 ppm aqueous solutions of xanthan gum (XG) and polyethylene oxide 200 kDa and 900 kDa.

Table 1. Interfacial properties of liquids

	Surface tension (mN/m)	Contact angle on amine modified surface (°)
Water	71.5	43
PEO 200k	62.0	40
PEO 900k	62.2	39
Xanthan gum	61.1	47

measured by an AR2000 rheometer (TA Instruments). XG solutions show shear-thinning behavior, while PEO solutions show almost constant viscosity. The surface tension of each liquid was also measured and found to be lowered about 20% at most as listed in Table 1. We used spherical particles of polystyrene (PS) with diameters of 1 and 6 μm. PS particles of 6 μm were polymerized by the dispersion polymerization, while PS particles of 1μm were polymerized by the emulsion polymerization. The average density of PS is 1,050 kg/m^3. Particles were washed more than 5 times with ethanol to eliminate the remaining monomer and surfactants and then dried. The dried particles were redispersed in liquids. In Fig. 2, microscopic images of the particles are shown. The PS particles are spherical and the size distributions are virtually monodisperse. We also purchased spherical particles of hollow glass spheres. According to

Table 2. Zeta potential of particles

	Zeta potential in water (mV)
Glass bead	−20.2±1.3
PS 1 μm	−19.8±1.2
PS 6 μm	−44.1±1.7

the manufacturer's specification, the particle size of hollow glass spheres is 9-13 μm and the average density is 1,100 kg/m^3. However, the glass sphere sample actually contains some small particles as shown in Fig. 2. Also, the surface of glass particles is not as smooth as PS particles. In suspending solid particles in water or polymer solutions, no surfactants were added since the particles were easily dispersed at least for a day. Also, we intended to eliminate the effect of additives except polymers. The zeta potentials of particles were measured using an electrophoretic light scattering spectrophotometer system with the standard zeta-potential cell unit (ELS8000, Otsuka Co.). In Tables 1 and 2 are listed the interfacial characteristics of base liquids and particles, respectively. The difference in zeta potential between 1 and 6 μm particles appears to be caused by the different polymerization method.

2. Drop Generation and Deposition on Solid

Suspension drops were generated by using a dispenser (EFD Ultra 2405) with a 25 gauge dispenser tip (inner diameter of the tip is 0.3 mm). A drop of liquid is squeezed out of the dispenser tip and falls down to the slide glass by gravity. The initial wetted diameter and drop height were approximately 2 mm and 0.8 mm, respectively. Since the initial distribution of particles within a drop can be different depending on impacting velocity of drop onto solid surface [17], the impacting velocity was chosen so that Weber number, the ratio of inertial force and surface tension force ($We=\rho U^2 d/\gamma$), was less than 1. The distance between the dispenser tip and the slide glass was 1 mm. The impact velocity onto the slide glass was estimated to be 0.2 ms^{-1}. In this case the impacting velocity is sufficiently small and the drop is spread by the capillary spreading mechanism. All the experiments were performed at room condition. Drying patterns were recorded using a CCD camera (Imperx IPX 2M30-L) controlled by Labview™ software. The pictures were taken every 2 seconds from below with a Nikon Zoom lens (50 mm, 1 : 1.4D) equipped with a 60 mm extension tube for close-up views. The dispenser tip was set on a homemade fixture which was connected to

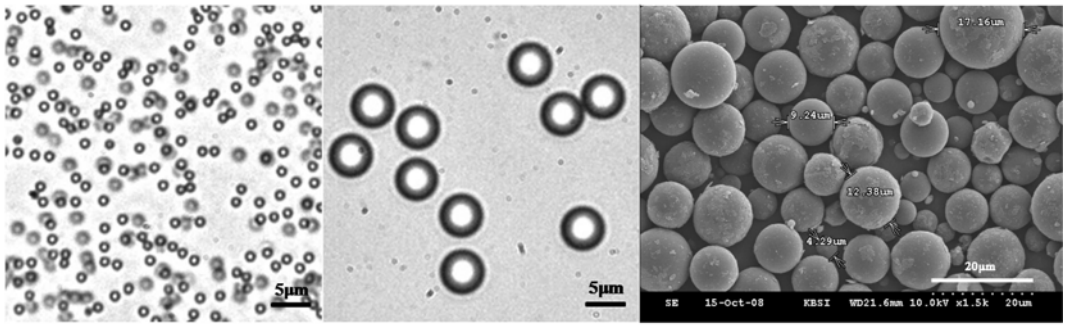

Fig. 2. The optical microscopic images of particles: (a) PS 1 μm; (b) PS 6 μm; (c) Glass bead.

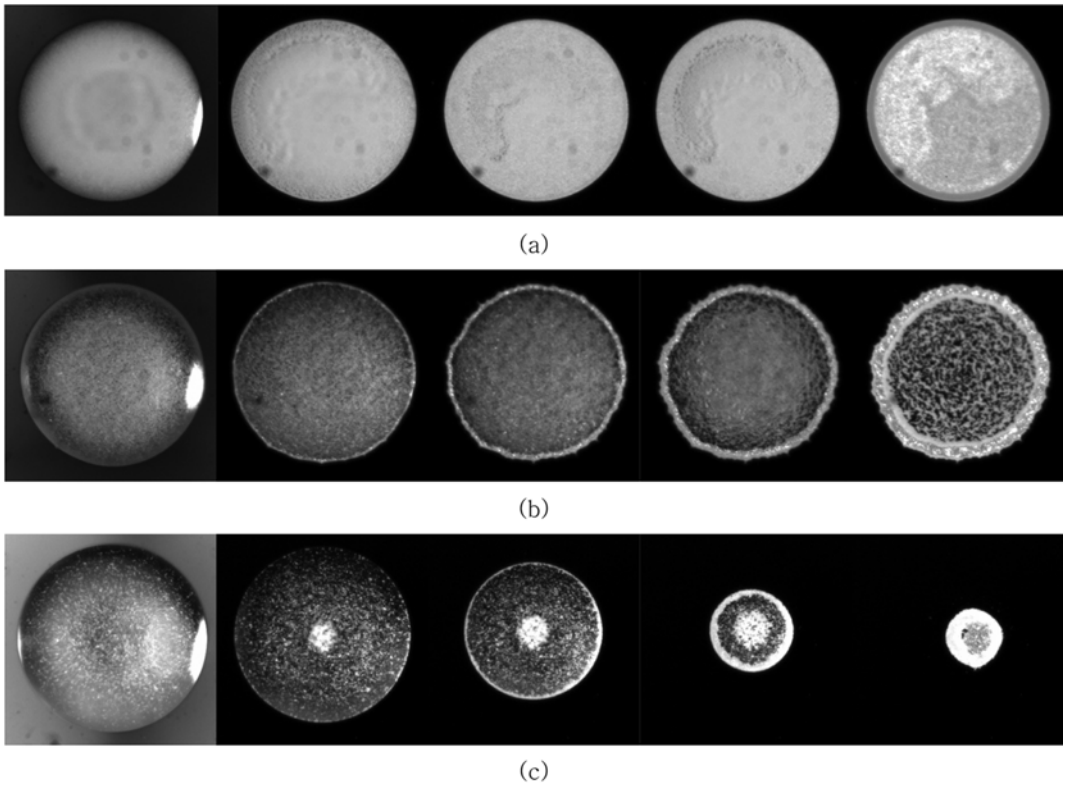

Fig. 3. The evolution of drying pattern of particle dispersed water: (a) PS 1 μm at 4, 200, 400, 600, 678 sec; (b) PS 6 μm at 4, 200, 400, 600, 682 sec; (c) Glass bead at 4, 200, 400, 600, 692 sec.

a motorized stage (Parker GV6 servomotor). No illumination was used to take images. The room temperature and relative humidity were 24-25 °C and 20%, respectively.

RESULTS AND DISCUSSION

1. Drying of Sessile Drops of Newtonian Fluid

Even though the purpose of the present research is to investigate the effect of added polymers on drying patterns the sessile drops of Newtonian fluid were dried first. This result will be the control for the non-Newtonian drop drying result. Fig. 3 shows the change in the drying pattern of Newtonian suspensions with time. In the case of 1 μm PS particles, particles move toward the rim as expected and the final drying pattern shows the coffee ring. Some particles are observed inside the coffee ring. This point will be considered later. In the case of 6 μm PS, however, no such pattern is observed. Particles move to the rim, but the rim is not pinned and recedes with time from the initially wetted perimeter. Due to this motion the rim is not smooth. Some particles are accumulated at the rim, but a substantial amount of particles remain inside the rim. Also, there is an almost particle-free region between the edge and the particle-scattered region just before the end of drying process (at 600 s). This means that there is a movement of particles toward the center as well as the outward movement by the Deegan flow. Fig. 3 also shows the drying patterns of glass beads of 9-13 μm. In this case the contact line is not pinned and the particles are almost uniformly distributed in the final drying pattern. Recently, Sangani et al. [18] reported that depending on particle size and particle concentration the contact line can pin or depin. Specifically, the contact line tends to pin when the particle size is smaller and particle concentration is larger. In the case of glass spheres the small particles mixed in the large particles do not seem to have strong enough role in pinning the contact line, and the large particles are dragged by the receding contact line. One thing we may note in Fig. 3 is that some glass beads move toward the center until they move toward the rim by the Deegan flow at the final stage when the contact angle at the rim becomes sufficiently small, and hence the flux becomes large. It has been confirmed, by changing the focus of the microscope, that the particles moving toward the center move along the air-liquid interface. The movement of particles captured at the interface seems to carry the suspension beneath the interface. It has been well known that some particles are captured at the air-liquid interface [19,20]. Dominguez et al. [21] reported that when a particle captured at the air-liquid interface is not fixed at the apex of the drop, there may exist a force pushing the particle toward the apex due to the force asymmetry except at the apex. Even though the origin of the force is unknown, it is certain that the inward movement of particles can change the drying pattern. There may be some lighter particles than water in the case of hollow spheres even though the average density of particles is 1,100 kg/m^3. In this case particles can rise to the surface and move to the center along the air-liquid interface. This result in the same movement is caused by the movement of particles by the surface force. The existence of particles moving toward the center will be utilized in probing the effect of added polymers.

2. Drying of Sessile Drops of PEO Solutions

Next, we consider the drying of particulate suspensions in poly-

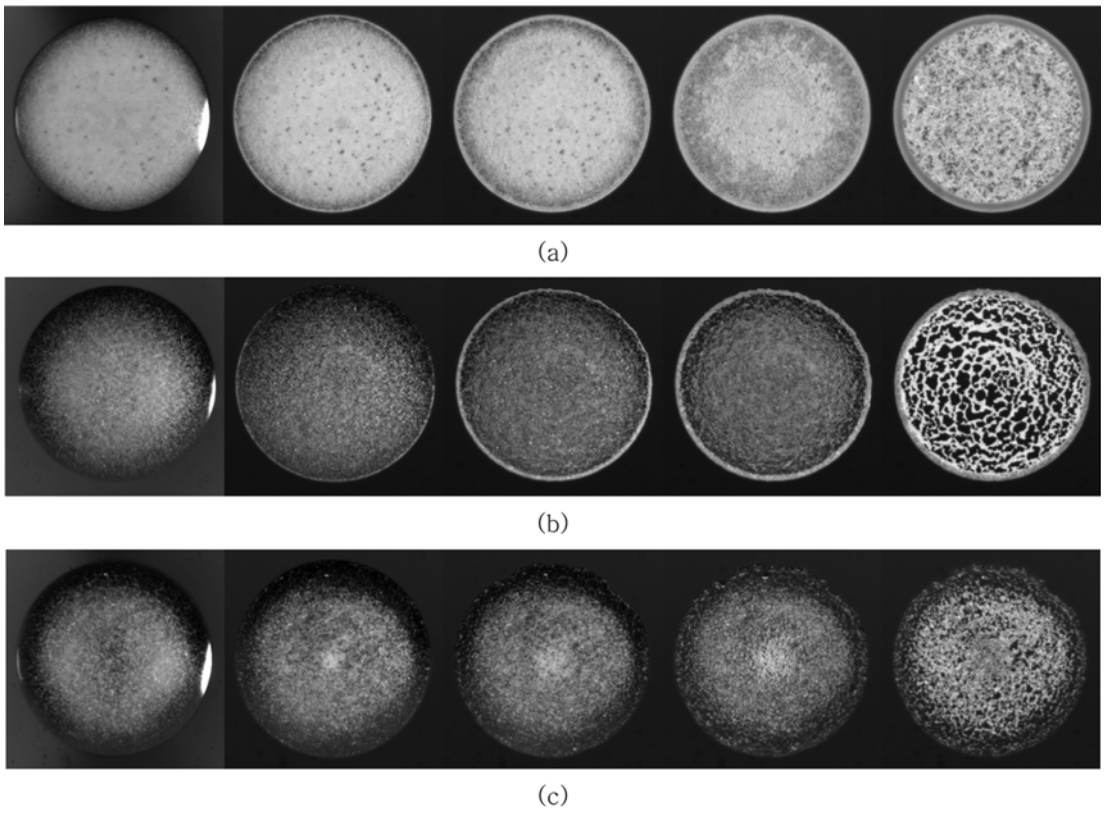

Fig. 4. The evolution of drying pattern of particle dispersed PEO200k solution: (a) PS 1 μm at 4, 100, 200, 300, 352 sec (b) PS 6 μm at 6, 100, 200, 250, 290 sec; (c) Glass bead at 6, 100, 200, 300, 338 sec.

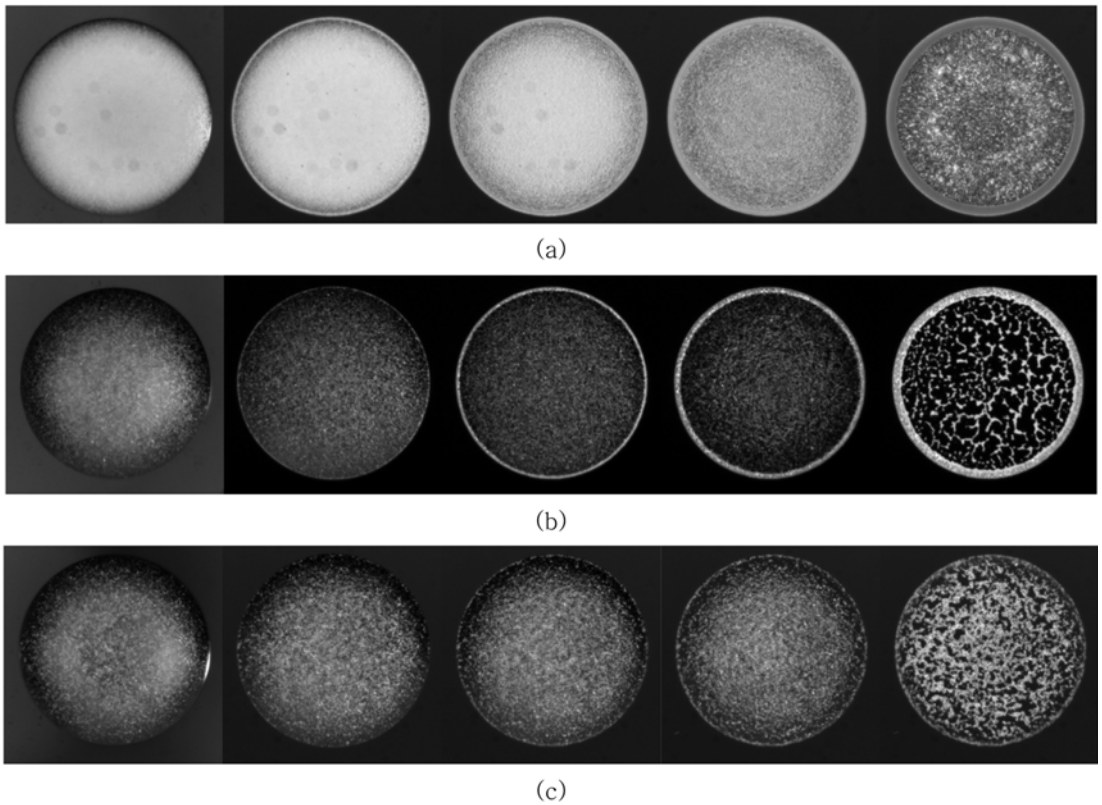

Fig. 5. The evolution of drying pattern of particle dispersed PEO900k solution: (a) PS 1 μm at 6, 100, 200, 250, 290 sec; (b) PS 6 μm at 6, 100, 300, 500, 556 sec; (c) Glass bead at 6, 100, 200, 300, 394 sec.

mer solutions. Figs. 4 and 5 show the drying process of suspensions of PS 1 μm, PS 6 μm and glass beads suspended in the aqueous solution of PEO 200 kDa and PEO 900 kDa, respectively. In the case of PS 1 μm and PS 6 μm, the drying processes are much the same. Considering that the Zimm relaxation times of PEO 200 kDa and PEO 900 kDa are much different (9.1 μs and 127 μs, respectively), one may argue that the elastic effect of polymers does not strongly affect the drying process. Here we calculated the Zimm relaxation time from the intrinsic viscosity ($\lambda=([\eta_0]\eta_s M_w)/R_gT$). In the case of PS 6 μm, the drying processes of PEO solutions are quite different from that of water. The most distinct difference is the contact line pinning in the case of PEO solutions. One may argue that some polymer molecules can be deposited upon drying at the early state of drying to pin the contact line. However, when PEO solutions were dried without particles, the contact line pinning characteristics were changed as shown in Fig. 6. In the case of PEO200k the pinning is very weak. In the case of xanthan gum it is not pinned. Only the contact line for PEO900k is pinned. This means that the deposition of polymer molecules by instantaneous drying at the contact line may not be the sole reason for the pinning. This also implies that the elasticity of polymers has a strong effect on pinning, and hence the pinning of the contact line for PS 6 μm in PEO solutions should be caused by the interfacial-hydrodynamic interaction among solid substrate, liquid and PS particles. Since Sangani et al.'s analysis [21] is for Newtonian fluids, it is not possible to apply their theory to our case. It requires the theory of the contact-line movement of viscoelastic fluids which has not been understood yet; hence the detailed reasoning for the difference may not be possible as of now.

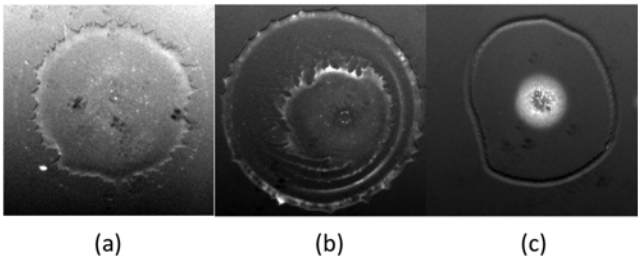

Fig. 6. The final drying patterns of polymer solutions without particles: (a) PEO 200k; (b) PEO 900k; (c) Xanthan gum.

In the case of 9-13 μm glass particles in the PEO solutions, the drying characteristics are different from that of the glass bead suspension in the Newtonian liquid. When a drop containing particles is spread on the solid surface, the glass beads are well distributed. As drying progresses the beads move toward the center until when about one half of the fluid is dried. Then some of the beads that are captured at the air-liquid interface and gathered at the central part move outward rapidly (in a time scale of 10 s, not shown in the Fig. 4). This is quite different from the Newtonian case in which particles stay at the center until the end of drying process. Also, the contract line is pinned at the initial perimeter. Again, there should be a strong interaction at the contact line to pin as in the case of PS 6 μm particles. In the final drying pattern, particles appear to be evenly distributed due to the change in the direction of movement of particles. The change of moving direction appears to be caused by the following reason. It is estimated that the average polymer concen-

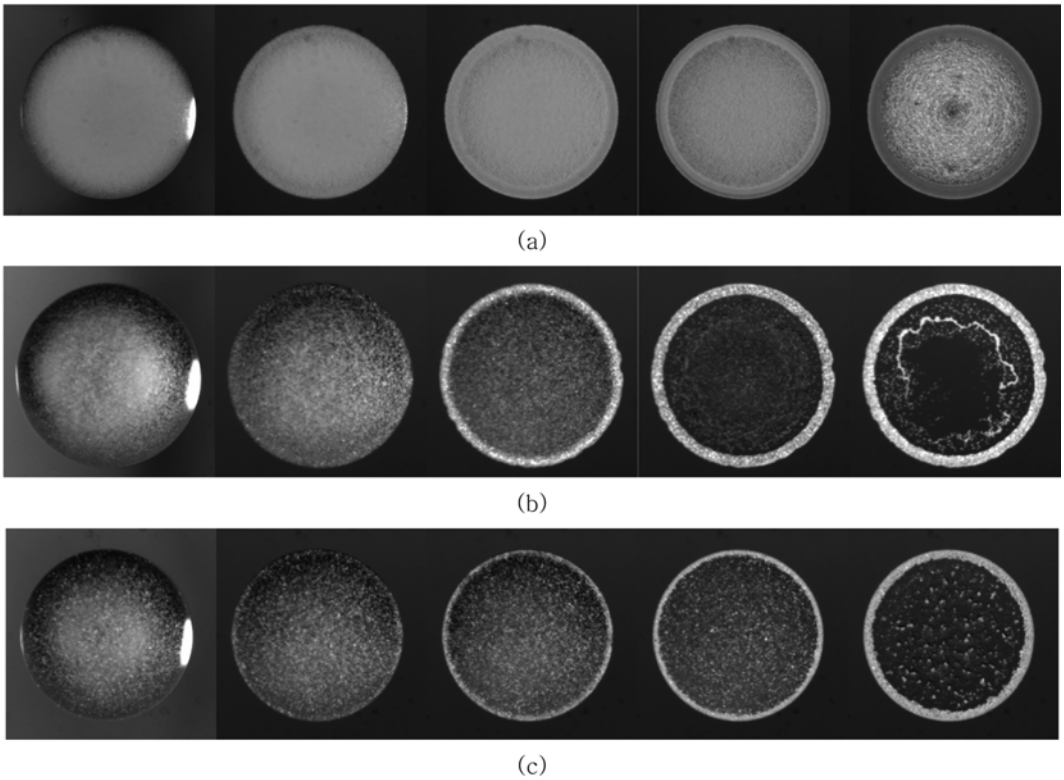

Fig. 7. The evolution of drying pattern of particle dispersed xanthan gum solution: (a) PS 1 μm at 6, 100, 300, 400, 524 sec; (b) PS 6 μm at 4, 100, 300, 400, 418 sec; (c) Glass bead at 6, 100, 200, 300, 400 sec.

tration inside the drop at the time of changing direction is approximately 2,000 ppm if the theoretical analysis by Hu and Larson [22] is applied. It was also confirmed by the measurement of the mass of drop as a function of time. At this condition, the zero shear viscosity of the polymer solution is not far from that of the solvent because the polymer concentration is far below the coil overlap concentration. If this is the case, there appears to be no reason why the direction has to be changed. However, the concentration of polymer should not be uniform due to its low diffusivity in liquid. Based on the dilute solution theory the diffusivity of single polymer molecules, $D=kT/6\pi a\eta_s$, is estimated to be 4×10^{-12} m^2s^{-1} (Here we assumed that the solution is in the dilute regime since the viscosity of polymer solution is less than twice the solvent viscosity. Then the intrinsic viscosity can be estimated. The radius of a single polymer molecule, a, is determined from the intrinsic viscosity). Then, the distance of the one-dimensional diffusion of polymer $\sqrt{2Dt}$ during half of the drying time is 30 μm, which is much shorter than the height of the drop. Therefore, the surface of the drying drop has much higher polymer concentration than the average polymer concentration and the viscous force due to the Deegan flow overcomes the surface force that holds the particles at the center since the skin region has a much higher viscosity. One may suspect the role of elasticity of polymers. But the elastic effect cannot be important, since the shear rate is approximately in the range of 0.001-0.01 s^{-1} except at the final stage of drying.

3. Drying of Sessile Drops of Xanthan Gum Solutions

In the case of xanthan solution, all kinds of particles tested here move toward the contact line as shown in Fig. 7. Since the drying occurs under very low shear conditions, the shear thinning property of xanthan solution that shows for many decades of shear rate may not be responsible directly because the Deegan flow occurs only under low shear rate regimes. Rather, the high viscosity of the solution at low shear rate appears to cause the movement. Since the average shear rate has an order of 10^{-3} s^{-1} and the shear rate at the position of 1 diameter away from the contact line is 0.3 s^{-1} (determined from Hu and Larson's velocity field [22]), the viscosity of 1,000 ppm XG solution is 500 times larger than the water viscosity, rendering the drag force much larger than the drag caused by water while keeping almost the same magnitudes in the surface tension force and drying rate because the low concentration of xanthan hardly changes the vapor pressure. (Here we considered the drag force at the position of 1 diameter away from the contact line to avoid the singularity at the contact line.) As shown in Fig. 7, we observe the outward movement of 9-13 μm glass beads, which is opposite to the Newtonian case. This result is not the same as the case of PEO solutions. The difference appears to be caused by the large zero shear viscosity. When zero shear viscosity is large, due to the Deegan flow with a large viscosity, particles that are captured at the air-liquid interface move toward the rim at the early stage, and hence there remain almost no particles to be moved at the later stage In XG solutions of lower concentrations, the outward movement becomes weaker and the contact line is not pinned. As shown in Fig. 8, in 500 ppm solutions, the result looks almost the same as 1,000 ppm case; in 250 ppm case some particles move outward while others do not and the contact line is slightly depinned; in 125 ppm solutions, the particle distribution becomes almost uniform. The series of experiments with xanthan solutions confirm that the large shear stress even at low shear rate causes the outward motion. The contact line tends to be pinned with increasing xanthan gum concentration. According to Sangani et al. [18], the criterion for contact line pinning is strongly dependent on capillary number, hence the viscosity. Since the viscosity of the 1,000 ppm xanthan gum solution is order of magnitude higher than the viscosity of water, there should be a strong tendency to pin the contact line. But as the concentration becomes lower the contact line tends to be depinned and in the case of the 62.5 ppm solution the contact line is not pinned and becomes very unstable.

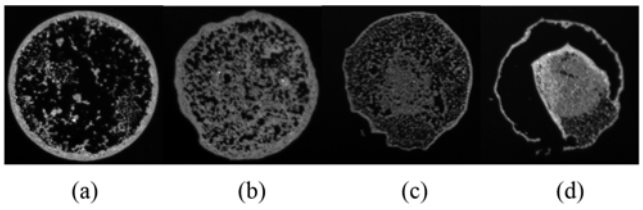

Fig. 8. The final drying patterns of xanthan gum solutions in water dispersed with glass beads: (a) Xanthan gum concentration of 500 ppm (b) 250 ppm (c) 125 ppm (d) 62.5 ppm.

4. Residues Left Inside the Rim

The amount of particles remaining inside the rim changes depending on particles and liquid. In the present study the glass substrate is positively charged while all the particles are negatively charged. Even though the charge density is not large, there should be some electrostatic interactions between the solid substrate and the particles. Due to the electrostatic interactions some particles are deposited on the solid substrate as shown in the Figs. 4 and 5. It appears that the reason that the deposition is most conspicuous in the case of PS 1 μm particles is caused by the small hydrodynamic stress due to the Deegan flow which drags the particle to the rim compared to the larger particles. In the case of xanthan gum solutions the drag force is very large due to its large zero shear viscosity. Therefore, there remains only a small amount of deposits.

CONCLUSION

We performed a series of drying experiments for suspension of various particle sizes in polymer solutions. The present experimental results reveal that, by controlling the drag force, we can control the drying pattern of sessile drops of particle-laden fluids on solid surfaces. This can be done by adding a small amount of macromolecules which bring high viscosity change with a negligible change in vapor pressure not to lower the evaporation rate. Elasticity of polymer solutions may not be a direct controlling variable even though it can change the pinning characteristics at the contact line. Changes in temperature or humidity may not be an effective way of controlling the final pattern. These changes will affect the final pattern only slightly by an indirect way such as the change in viscosity and surface tension, which may not be large enough to change the system on a qualitative scale.

ACKNOWLEDGEMENT

This work was supported by Project Number D00188 (in 2008) from the Basic Research Program of the Korea Research Foundation (National Research Foundation of Korea). The authors thank

Professor Sung Jae Lee for providing the PS particles.

NOMENCLATURE

a : polymer radius [m]
d : drop diameter [m]
D : diffusivity [m^2s^{-1}]
k : Boltzmann constant [$J \cdot K^{-1}$]
M_w : molecular weight [$kg \cdot mol^{-1}$]
t : time [s]
R_g : gas constant [$J \cdot mol^{-1} \cdot K^{-1}$]
T : temperature [K]
U : velocity [$m \cdot s^{-1}$]
We : Weber number [-]
γ : surface tension [$N \cdot m^{-1}$]
η_s : viscosity of solvent [Pa·s]
$[\eta_0]$: intrinsic viscosity [$m^3 \cdot kg^{-1}$]
ρ : density [$kg \cdot m^3$]

REFERENCES

1. I. Viola, F. D. Sala, M. Piacenza, L. Favaretto, M. Gazzano, M. Anni, G. Barbarella, R. Cingolani and G. Gigli, *Adv. Mater.*, **19**, 1597 (2007).
2. F. L. Yap and Y. Zhang, *Biomaterials*, **8**, 2328 (2007).
3. D. J. Harris, H. Hu, J. C. Conrad and J. A. Lewis, *Phys. Rev. Lett.*, **98**, 148301 (2007).
4. A. M. J. van den Berg, A. W. M de Laat, P. J. Smith, J. Perelaer and U. S. Schubert, *J. Mater. Chem.*, **17**, 677 (2007).
5. B. J. de Gans, S. Hoeppener and U. S. Schubert, *J. Mater. Chem.*, **17**, 3045 (2007).
6. R. D. Deegan, O. Bakajin, T. F. Dupont, G. Hueber, S. R. Nagel and T. A. Witten, *Nature*, **389**, 827 (1997).
7. H. Hu and R. G. Larson, *Langmuir*, **21**, 3972 (2005).
8. W. D. Ristenpart, P. G. Kim, C. Domingues, J. Wan and H. A. Stone, *Phys. Rev. Lett.*, **99**, 234502 (2007).
9. K. Uno, K. Hayashi, T. Hayashi, K. Ito and H. Kitano, *Colloid Polym. Sci.*, **276**, 810 (1998).
10. B. Y. Tay and M. J. Edirisinghe, *Proc. Roy. Soc. Lond. A*, **458**, 2039 (2002).
11. Q. Yan, L. Gao, V. Sharma, Y. Chiang and C. Wong, *Langmuir*, **24**, 11518 (2008).
12. R. Bhardwaj, X. Fang, P. Domsdundaran and D. Attinger, *Langmuir*, **26**, 7833 (2010).
13. R. Bhardwaj, X. Fang and D. Attinger, *New J. Phys.*, **11**, 1 (2009).
14. C. H. Chon, S. Paik, J. B. Tipton Jr. and K. D. Kihm, *Langmuir*, **23**, 2953 (2007).
15. E. R. Lee, *Microdrop generation*, CRC Press, Boca Routon (2003).
16. J. A. Lewis, *J. Am. Ceram. Soc.*, **83**, 2341 (2000).
17. M. Nikolas, *J. Fluid Mech.*, **545**, 271 (2005).
18. A. S. Sangani, C. Lu and J. A. Schwarz, *Phy. Rev. E*, **80**, 011603 (2009).
19. A. V. Rapacchietta, A. W. Newmann and S. N. Omenyi, *J. Colloid Interface Sci.*, **59**, 541 (1977).
20. A. V. Rapacchietta and A. W. Newmann, *J. Colloid Interface Sci.*, **59**, 555 (1977).
21. A. Dominguez, M. Oettel and S. Dietrich, *J. Chem. Phys.*, **128**, 114904 (2008).
22. H. Hu and R. G. Larson, *Langmuir*, **21**, 3963 (2005).